1990-08

Schlieren Studies of Compressibility Effects on Dynamic Stall of Airfoils in Transient Pitching Motion

Chandrasekhara, M.S.; Ahmed, S.; Carr, L.W.

8th Applied Aerodynamics Conference August 20-22, 1990/Portland,Oregon
http://hdl.handle.net/10945/50450

AIAA-90-3038

Schlieren Studies of Compressibility Effects on Dynamic Stall of Airfoils in Transient Pitching Motion

M.. Chandrasekhara, Naval Postgraduate School, Monterey, CA;
S. Ahmed, MCAT Institute, San Jose, CA;
L. Carr, NASA-Ames, Moffett Field, CA

8th Applied Aerodynamics Conference
August 20-22, 1990/Portland, Oregon

Schlieren Studies of Compressibility Effects on Dynamic Stall of Airfoils in Transient Pitching Motion

M.S.Chandrasekhara [1]
Navy-NASA Joint Institute of Aeronautics
Department of Aeronautics and Astronautics
Naval Postgraduate School, Monterey, CA 93943

S.Ahmed [2]
Navy-NASA Joint Institute of Aeronuatics and
MCAT Institute, San Jose, CA

and

L.W.Carr [3]
Aeroflightdynamics Directorate, U.S.Army ARTA and,
Fluid Dynamics Research Branch
Fluid Mechanics Laboratory
NASA Ames Research Center, Moffett Field, CA 94035

Abstract

Compressibility effects on the flowfield of an airfoil executing rapid transient pitching motion from 0 - 60 degrees over a wide range of Mach numbers and pitching rates were studied using a stroboscopic schlieren flow visualization technique. The studies have led to the first direct experimental documentation of **multiple shocks** on the airfoil upper surface flow for certain conditions. Also, at low Mach numbers, additional coherent vortical structures were found to be present along with the dynamic stall vortex, whereas at higher Mach numbers, the flow was dominated by a single vortex. The delineating Mach number for significant compressibility effects was 0.3 and the dynamic stall process was accelerated by increasing the Mach number above that value. Increasing the pitch rate monotonically delayed stall to angles of attack as large as 27 degrees.

Nomenclature

c	airfoil chord
M	free stream Mach number
U_∞	free stream velocity
x	chordwise distance
α	angle of attack
$\dot{\alpha}$	pitch rate, degrees/sec
$\alpha^+ = \frac{\dot{\alpha}c}{U_\infty}$	nondimensional pitch rate

[1] **Assistant Director and Adjunct Research Professor, Assoc. Fellow AIAA.**

[2] **Research Scientist.**

[3] **Research Scientist and Group Leader, Unsteady Viscous Flows, Member AIAA.**

1. Introduction

There is considerable interest in the enhancement and sustenance of lift by dynamically pitching an airfoil in applications related to fixed wing aircraft supermaneuverability and enhanced agility. The production of dynamic lift by rapid unsteady motion such as oscillatory pitching or ramp type pitching is well known. Carr[1] provides a comprehensive review of the problem and related processes. Over the years, significant effort has been devoted to obtaining details of the process of dynamic lift generation over a rapidly pitching airfoil, quantify it and identify the parameters affecting it[2]. A survey of the available literature reveals that the process of dynamic stall is strongly dependent on the airfoil geometry (in particular the leading edge shape), Mach number, degree of unsteadiness or nondimensional pitch rate, Reynolds number, state of the airfoil boundary layer, airfoil initial angle of attack before pitching, three dimensionality, type of airfoil motion, location of pitch point, etc. The various aspects of the problem have been studied by several researchers. Freymuth[3] provides excellent flow visualization pictures at low speeds. Lorber and Carta[4], Albertson et al[5], Walker et al[6], among others have measured the surface pressure distributions. Francis and Keese[7] have found that the maximum lift coefficient increases monotonically till a nondimensional pitch rate of 0.025 and decreases therafter. Jumper et al[8] concluded from their studies that the pitch point has a large effect on dynamic stall. Harper and Flanigan[9] found that as the Mach number is increased, the dynamic lift steadily decreases and finally ceases at M $\approx$ 0.6 . Whereas these above mentioned studies are experimental, there are some computational studies (Ekaterinaris[10], Visbal[11], among others) that have produced good agreement with the available data.

The phenomenon of dynamic stall is characterized primarily by a clockwise vortex (for flow moving from left to right) that is produced by the large amount of coherent

vorticity that is created near the leading edge region of rapidly pitching airfoils by the unsteady motion. In fact, for certain flow conditions, Walker et al[6] observed that two vortices are present on the airfoil. During the early stages of the stall process the flow around the airfoil remains attached, with the vortex being surrounded by the outer stream. As the angle of attack is increased well past the static stall angle, the vortex begins to convect over the upper surface and grows. Eventually, when the vortex is shed into the wake, deep dynamic stall is said to occur. This sequence of events has been derived from flow visualization experiments at low Mach nmubers. Computations and surface presure measurements have shown that extremely large suction pressures develop in the region very close to the leading edge, pointing to formation of locally supersonic regions. In fact, even at the low free stream Mach number of 0.2, the local flow can attain sonic values[12]. It is then likely that a shock can form in the flow. If it does, it could have a dramatic effect on the dynamic stall process. However, till now there has been no direct experimental evidence of a shock, although its presence has been inferred from other measurements such as signatures of surface mounted hot film gages[4]. It is very clear that there is a strong need to obtain detailed experimental data about the influence of compressibility effects on dynamic stall before a full understanding of the dynamic stall process can be obtained. This paper presents some of the results of a visualization of the flow carried out using a stroboscopic schlieren method.

2. Description of the Experiment

A. Facility

The experiments were conducted in an in-draft wind tunnel of the Fluid Mechanics Laboratory (FML) at NASA Amers Research Center (ARC). It is one of the ongoing dynamic stall research projects of the Navy-NASA Joint Institute of Aeronautics between the Naval Postgraduate School and NASA ARC.

The details of the FML in-draft wind tunnel are given in Carr and Chandrasekhara [11]. The facility is one of a complex of four in-draft wind tunnels connected to an evacuation compressor. The test section size is 25cm X 35cm X 100cm. The flow in the tunnel is controlled by a variable cross section throat downstream diffuser. The throat is always kept choked so that no disturbances can propagate from the other tunnels or the compressor into the test section.

An NACA 0012 airfoil with a chord of 7.62cm is supported in a unique way by pins that are push fitted between two 2.54cm. thick optical quality glass windows. The pins are smaller than the local airfoil thickness and hence permit complete optical access to the airfoil surface. This makes detailed flow studies possible even at the surface. The airfoil motion is produced by a hydraulic drive located on top of the test section, which is connected to the window frames supporting the airfoil. Controlled movement of the hydraulic actuator provides the desired motion of the airfoil. Fig. 1 shows a schematic of the tunnel with the drive system.

B. Details of the Hydraulic Actuator System

The following were specified as the requirements on the airfoil motion:

angle of attack, α:	0-60°
pitch rate, $\dot{\alpha}$:	0-3600 °/sec
acceleration rate:	600,000 $°/sec^2$
change in α during acceleration:	$\leq$6° of pitch
acceleration time:	4 milliseconds
free stream Mach number:	0.1-0.5
airfoil chord:	7.62cm
Reynolds number:	2 x 10^5 - 10^6

It should be noted that at any Mach number, a 7.62cm chord airfoil pitching at 3600^0/sec. corresponds to a 3m chord wing pitching at 90^0/sec., which is beyond the range of present day aircraft. Thus, results obtained from this study will enable expanding the flight envelope of both current and future aircraft systems. The acceleration time was limited to 4 milliseconds and the change in angle of attack during this time was specified to be less than 6^0 so that the airfoil has reached a constant pitch rate well before the static angle is reached. To obtain reasonable experiment times, the system was also required to recycle 30 times a minute.

These exacting requirements meant that a powerful prime mover was necessary for this purpose. After considering several alternatives, a hydraulic drive system was found to be able to deliver the required performance. Such a system was designed taking into account the fact that the system characteristics are collectively determined by the interaction of the aerodynamic flow field, the mechanical system with its linkages and associated backlash, and the hydraulic system with its leakage and the nonlinearities in each of these systems. The details of the feed back system design can be found in Andrews[14]. Chandrasekhara and Carr[15] provide the other details of the final design, including those of the hydraulic circuit.

C. Instrumentation and Technique

The drive is equipped with its own instrumentation which is used by the feed back control system. These include a digital incremental position encoder (with a resolution of 0.03^0/count) to provide the instantaneous angle of attack, and a linear (analog) velocity transducer for maintaining the airfoil velocity constant. The airfoil motion is software controlled from an IBM PC, with a motion controller card installed in one of its slots.

As stated earlier, the airfoil pitches from 0 - 60^0 at pitch rates up to 3600^0/second and the motion is completed in 20 milliseconds. Records of individual pitch up motion were obtained using a MicroVAX II Work Station. The PC was linked to the MicroVAX with additional hardware to trigger data acquisition on the MicroVAX computer, using the third bit of the encoder providing the instantaneous angle of attack information. The third bit was chosen to prevent accidental triggering due to noise or such uncontrollable parameters. Simultaneously, the internal clock of the computer was started so that the time history of the motion could be documented. Fig. 2 shows typical plots of the variation of angle of attack with time for M = 0.45, a pitch rate $\dot{\alpha}$, of 3507^0/sec, and nondimensional pitch rate $\alpha^+ = 0.03$; M = 0.35, $\dot{\alpha} = 2256^0$/sec.,

$\alpha^+ = 0.025$; and M = 0.25, $\dot{\alpha} = 1263^0$/sec, $\alpha^+ = 0.02$. Similar plots were obtained for all cases.

The schlieren instrumentation used is standard and is shown in Fig. 3. It is also described in Carr and Chandrasekhara[13]. Flow visualization was obtained using the stroboscopic schlieren flow visualization technique. This involved triggering the schlieren light source at the desired instantaneous angle of attack by a specially designed electronic circuit. The encoder counts for the desired angle of attack was chosen as a BCD number by setting switches on the front panel of the hardware. The circuit includes a comparator which outputs a TTL pulse when a match occurs between the selected count and the constantly changing encoder count. This pulse triggers the strobe light source and also freezes the display of the encoder counter, thus permitting a check on and recording of the actual angle of attack at which the light flashed. No phase delays were found to be present in this process.

The experiment consisted of running the tunnel at Mach numbers ranging from 0.2 - 0.45, while pitching the airfoil at rates from 1200 - 3600 degrees/sec., and taking the schlieren pictures. The resulting Reynolds number range was 400,00 - 900,000. The matrix of experimental conditions is given in Table 1.

3. Results and Discussion

A. Stroboscopic Schlieren Flow Visualization Studies

Fig. 4 and 5 present two sequences of stroboscopic schlieren pictures obtained for the cases of M = 0.25, $\alpha^+ = 0.05$ and M = 0.45, $\alpha^+ = 0.03$. These pictures were obtained by pitching the airfoil once for each frame shown. They represent the density gradients at the instant the pictures were taken without any history effects - unlike most other flow visualization photographs. The knife edge of the schlieren system was kept vertical for all cases.

The dominant feature in these figures is the presence of the dynamic stall vortex that appears as a dark circular region over the airfoil and moves along the airfoil upper surface and eventually past the trailing edge.

The dark region near the leading edge of the airfoil on its lower surface indicates the density gradients in the stagnating flow. As the angle of attack increases (up to 30^0), the stagnation point moves downstream along the lower surface and stabilizes at $\approx$ 5% chord point. Also, as the angle of attack in increased, the dynamic stall vortex becomes distinct at $\alpha = 17^0$ in Fig. 4 at M = 0.25 and $\alpha^+ = 0.05$, and $\alpha = 13^0$ for the case of the higher Mach number of 0.45 and $\alpha^+ = 0.03$ in Fig. 5. In both cases, the vortex quickly grows into a large coherent structure. The boundary layer downstream of the vortex thickens with increasing angle of attack; at the same time, the leading edge shear layer appears as a thin streak (starting out initially as a dark layer and transforming into a lighter shade) and delineates the outer potential flow from the inner separated viscous layer. Ultimately, the vortex is bounded by the edge of the shear layer upstream and by the boundary layer downstream. The flow downstream of the dynamic stall vortex is still attached,as can be seen, for example, in Fig. 5, $\alpha = 14.5^0$. No trailing edge vortex was present for any of the cases studied. Walker et al[6] have pointed out that the trailing edge vortex is due to the separating shear layer on the upper surface and is absent at higher Reynolds numbers, which is perhaps the reason why it was not found in the cases studied.

The vortex itself appears as a dark region as in its formative stages, the flow gradients in it have not fully developed. But, when it grows and has acquired its terminal velocity, it appears as a partially bright and partially dark image, with a sharp transition line where the local density gradient changes sign from negative to positive (light to dark), as can be seen in Fig. 4 for $\alpha = 21.0^0$. For the case shown in Fig. 4, the flow stalls dynamically at $\alpha = 27^0$ (when the vortex has travelled past the trailing edge) and for M = 0.45, (Fig. 5), at $\alpha = 18^0$. Both these angles are substantially higher than the corresponding static angles. (See also Table 2).

As the airfoil pitches past this angle, the flow becomes largely separated and the separating leading edge shear layer grows unstable forming several vortices, as can be seen from the bottom row frames in both Fig. 4 and Fig. 5. The flow downstream of the trailing edge also shows several small organized vortical structures. Occasionally, (Fig. 4, $\alpha = 28^0$) a trailing vortex (much like the starting vortex) can be seen coming off the trailing edge of the airfoil during the deep stall phase of the flow.

Fig. 6 presents an enlarged schlieren picture for M = 0.25, $\alpha^+ = 0.025$, at $\alpha = 16.5^0$. At this condition, some interesting details are present in the flow. As already stated, the forward stagnation point is on the lower surface at about 5%chord point. On the upper surface, there is a large dynamic stall vortex at x/c $\approx$ 0.5. Along with it it is another structure, which appears to have the same sense of vorticity as the dynamic stall vortex. Downstream of the primary vortex, the flow is still attached. It is surprising to see two clockwise vortical structures at the same time. Chandrasekhara et al[18] have detected such structures in their computational studies of the flow over an oscillating airfoil under compressibility conditions. Mane et al[19] have also found such structures in their computational studies on pitching airfoils, but at a low Reynolds number of 50,000. At this stage, it is not known whether the multiple structures would influence dynamic lift generation in any way. However, these seem to appear mostly at low Mach numbers and only at low pitch rates.

Another noteworthy feature is the large vertical length scale of the flow. It appears that the vortex diffuses and rapidly becomes disorganized as it moves over the airfoil. In contrast, studies of the flow field over an oscillating airfoil by Chandrasekhara and Carr[16] have shown that the vortex was very tightly wound. Chandrasekhara et al[17] have compared the effect of motion history and found that in the range of parameters tested, the ramp type motion is not very effective in introducing the levels of vorticity that can be attained by the oscillating motion due to the fact that the integrated effect of pitch rate history on vorticity generation is larger in the oscillating case. This is a possible explanation for the observed structure of the dynamic stall vortex in this case.

B. Formation of Shocks over the Airfoil

Fig. 7 shows the details of the flow near the leading edge of the airfoil for M = 0.45, $\alpha^+ = 0.0313$, $\alpha = 12.6^0$.

The strong density gradient near the airfoil leading edge under these conditions are responsible for deflecting the light rays completely around the region, which results in a dark region seen on the upper surface in this figure. The most striking result seen in the figure is the presence of multiple shocks within the first 5 - 8% chord distance. The rapid acceleration of the flow around the leading edge for this case has caused the flow to go supersonic. Such a result has also been indicated in computational studies. The extent of the supersonic region depends upon the Mach number, nondimensional pitch rate and instantaneous angle of attack. For example, Visbal[11] found that a supersonic region originates very near the leading edge and extends till about 8 - 10% chord point for M = 0.3, and it grows to about 30% chord at M = 0.6. The results obtained from the present study offer the first definitive experimental documentation of the fact that shocks actually form on the airfoil for certain flow conditions and support the study by Visbal[11]. It is well known that once a flow attains supersonic values, a shock can form. In the present case, it is not known whether the shock is normal or oblique, but presence of multiple shocks indicates that if a normal shock orignally formed, there are additional mechanisms present in the flow that are responsible for accelerating the flow repeatedly to supersonic values and thus forming more shocks. A possible explanation is that the shock induces small scale separation in the boundary layer. The separating streamlines could take a wavy shape and thus locally induce a series of expansion and compression waves. Such a system of waves could form additional shock waves (or shocklets) in the flow. Eventually the series of interactions ceases via a 'strong' shock and the flow becomes subsonic. This explanation still needs to be verified, but such a situation seems possible in transonic flow. Meier[20] has observed multiple shocks in vortex-wing interaction studies in transonic flows.

The shocks discussed above were present over a range of angles of attack and flow conditions. A sequence of schlieren pictures for M = 0.45, at a pitch rate of 3600 degrees/sec. ($\alpha^+ = 0.0313$) is presented in Fig. 8. These were obtained at a very fine resolution over angles of attack ranging from 12.2^0 - 12.9^0. It can be seen that at $\alpha = 12.4^0$, shocks (the thin dark streaks in the figure) appear over the airfoil surface in the region x/c = 0 - 0.05. At $\alpha = 12.4^0$, several shocks form and extend 1 - 2% chord width into the upper surface flow. The shocks remain on the surface at $\alpha = 12.5^0$. At $\alpha = 12.7^0$, only a single "strong" shock remains at about 10% chord, just upstream of the dark region. The shock finally disappears at an angle of attack of 13^0. However, no large scale shock induced separation could be detected for the cases studied. In fact, the dynamic stall vortex still forms and eventually gets shed at $\alpha = 17^0$.

C. Effect of Mach Number

Fig. 9 compares the schlieren pictures at different Mach numbers for $\alpha^+ = 0.03$ and $\alpha = 17^0$. It can be seen that for the subsonic case ($M \leq 0.3$), the vortex is at about 50% chord location. In addition, the vertical extent of the flow is nearly the same for M = 0.2, 0.25 and 0.3. However, for $M \geq 0.3$, the dynamic stall vortex moves successively closer to the trailing edge and the flow scales have increased as well. Movement of the vortex downstream indicates flow approaching the deep stall state and thus, it is clear from the figure that as the Mach number is increased, deep stall occurs at progressively lower angles of attack.

Fig. 10a shows the effect of Mach number on the dynamic stall for the pitch rate $\alpha^+ = 0.025$, and the corresponding results for $\alpha^+ = 0.035$ are shown in Fig. 10b. Plotted in it are the successive locations of the center of the dynamic stall vortex as a function of the instantaneous angle of attack at different Mach numbers. It can be seen in both the figures that the vortex appears at lower angles of attack as the Mach number increases. This also leads to the result that the vortex moves past the trailing edge at lower angles of attack for higher Mach numbers, causing deep dynamic stall to occur earlier in the pitching cycle. Significant decreases in the angle of attack occur for the same x/c location for $M \geq 0.3$ and thus, M = 0.3 can be considered to be the limit when compressibility effects set in. Consider for example Fig. 10a, for x/c, ≈ 0.6, the center of the vortex is at $\alpha = 16.5^0$ for M = 0.3, and $\alpha = 14^0$ for M = 0.45. Similarly, in Fig. 10b, the vortex is at 60% chord location at $\alpha = 19^0$ for M = 0.3; at M = 0.4, the corresponding angle of attack = 17.2^0. Similar results were obtained at other pitch rates.

Table 2 shows the angle of attack at which deep dynamic stall occurs for the cases studied. As the Mach number is increased for a given pitch rate, the dynamic stall angle remains nearly the same up to M = 0.3. However, for $M \geq 0.3$, this angle decreases. The scatter that is present in the data is unavoidable, owing to the subjectiveness involved in determining these angles. Further, as already stated in Section 3.A, for some cases multiple structures were found to be present. This, along with the diffused vortex, made the task of tracking the vortex movement more complex. Nevertheless, the data shows definitive trends that reflect the compressibility effects.

D. Effect of Pitch Rate

Fig. 11a through 11d show the vortex center locations over the airfoil plotted as a function of the angle of attack at different pitch rates for M = 0.2, 0.35, 0.4 and 0.45 respectively. It can be seen in all the figures that the vortex is retained on the surface of the airfoil to higher angles of attack as the pitch rate is increased. The trend is monotonic with increasing pitch rate. For example at M = 0.45, the vortex is on the surface even at $\alpha = 18^0$ at $\alpha^+ = 0.03$, whereas the static stall angle for this case is $\approx 9.5^0$ as determined from the schlieren images. For $\alpha^+ = 0.020$, deep dynamic stall occurs at $\alpha = 15.5^0$. For M = 0.35, the deep stall angle is $\approx 23^0$ for $\alpha^+ = 0.04$, and the static stall angle is 11.6^0. The figures show similar results for other Mach numbers. A summary of dynamic stall angles is presented in Table 2 at different pitch rates. A horizontal scan of the table shows stall delay till angles of attack significantly higher than the static stall angles can be achieved by simply increasing the nondimensional pitch rate, even at these higher Mach numbers. As indicated in the previous section, presence of multiple structures, especially at the low Mach number of 0.2, made following the primary vortex during its passage over the airfoil difficult. Hence, the plot for $\alpha^+ = 0.025$ in Fig. 11a does not extend till the deep stall angle of attack.

4. Concluding Remarks

Results obtained showing the global behavior of the dynamic stall vortex over an airfoil executing a rapid transient pitching motion are presented. These are the first pictures of the flowfield obtained at maneuver Mach number conditions and for conditions that are beyond the operational range of present day aircraft.

The following major conclusions could be drawn from the study.

1. Multiple shocks are present over the airfoil, at moderate free stream Mach numbers. The shocks do not seem to induce any large scale flow separation. Also, the global features of the dynamic stall process are not significantly affected by their presence. However, detailed studies are still needed to confirm local effects of the shocks.

2. At low Mach numbers, multiple vortices are present at low pitch rates. But, at higher Mach numbers, a single large dynamic stall vortex dominates the flow. Occasionally, a trailing vortex similar to the starting vortex is observed.

3. Compressibility effects are important for $M \geq 0.3$.

4. Stall delay is enhanced by increasing the pitch rate. Increasing Mach number accelerates dynamic stall by lowering the angle of attack at which dynamic stall occurs.

Acknowledgements

The project was supported by AFOSR-MIPR-87-0029 and 88-0010 (monitored by Capt. H.Helin) with additional support from NAVAIR (Mr. T. Momiyama) and ARO (Dr. T.L.Doligalski). The technical support of Mr. Michael J. Fidrich and the staff of the NASA Fluid Mechanics Laboratory is greatly appreciated.

5. References

[1] Carr,L.W., "Progress in Analysis and Prediction of Dynamic Stall", *Journal of Aircraft*, Vol.25, No.1, Jan. 1988, pp. 6-17.

[2] McCroskey, W.J., "The Phenomenon of Dynamic Stall", NASA TM 81264, March 1981.

[3] Freymuth, P., "Vortex Patterns of Dynamic Separation", *Encyclopedia of Fluid Mechanics*, Ed. N.P.Cheremisinoff, Gulf Publishing Corp., Vol. 8, 1989, Chapter 11.

[4] Lorber, P.F. and Carta, F.O., "Unsteady Stall Penetration Esperiments at High Reynolds Number", AFOSR-TR-87-1202, April 1987.

[5] Albertson, J.A., Troutt, T.R., and Kedzie, C.R., "Unsteady Aerodynamic Forces at Low Airfoil Pitching Rates", AIAA Paper No. 88-2579-CP.

[6] Walker, J.M., Helin, H.E., and Strickland, J.H., "An Experimental Investigation of an Airfoil Undergoing Large-Amplitude Pitching Motions", *Journal of Aircraft*, Vol. 23, No. 8, Aug. 1985, pp. 1141-1142.

[7] Francis, M.S., and Keese, J.E., "Airfoil Dynamic Stall Performance with Large-Amplitude Motions", *Journal of Aircraft*, Vol.23, No.11, Nov. 1985, pp. 1653-1659.

[8] Jumper, E.J., Dimmick, R.L., and Allaire, A.J.S., "The Effect of Pitch Location on Dynamic Stall", *Journal of Fluids Engineering, Trans. ASME*, Vol. 111, No. 3, Sep. 1989, pp. 256-262.

[9] Harper, P.W, and Flanigan, R.E. "The Effect of Rate of Change of Angle of Attack on the Maximum Lift of a Small Model", NACA TN 2061, March 1950.

[10] Ekaterinaris, J.A., "Compressible Studies of Dynamic Stall", AIAA Paper 89-0024, Jan. 1989.

[11] Visbal, M.R., "Effect of Compressibility on Dynamic Stall of a Pitching Airfoil", AIAA Paper No. 88-0132, Jan. 1988.

[12] McCroskey, W.J., McAlister, K.W., Carr, L.W., Pucci, S.L., Lambert, O., and Indergrand, R.F., "Dynamic Stall on Advanced Airfoil Sections", *Journal of American Helicopters Society*, Vol. 26, No. 3, pp. 40-50.

[13] Carr, L.W., and Chandrasekhara, M.S., "Design and Development of a Compressible Dynamic Stall Facility", AIAA Paper No. 89-0647, Jan. 1989.

[14] Andrews, D.R., "An Airfoil Pitching Apparatus: Modelling and Control Design", 35th ISA International Instrumentation Symposium, Orlando, Fl, May 1989.

[15] Chandrasekhara, M.S. and Carr, L.W, "Design and Development of a Facility for Compressible Dynamic Stall Studies of a Rapidly Pitching Airfoil", *Proceedings of the 15th ICIASF Conference*, Goettingen, West Germany, Sept. 18-21, 1989.

[16] Chandrasekhara, M.S., and Carr, L.W., "Flow Visualization Studies of the Mach Number Effects on the Dynamic Stall of an Oscillating Airfoil", AIAA Paper No. 89-0023, Jan. 1989. (also to appear in *Journal of Aircraft*, Vol. 28, No. 7, July 1990.)

[17] Chandrasekhara, M.S., Carr, L.W., and Ahmed, S. , "Comparison of Pitch Rate History Effects on Dynamic Stall", *Proceedings of NASA/AFOSR/ARO Workshop on Physics of Forced Unsteady Separation*, April 1990.

[18] Chandrasekhara, M.S., Ekaterinaris, J.A., and Carr, L.W., "Experimental and Computational Tracking of Dynamic Stall Vortex", *Bull. American Physical Society*, Vol. 33, No. 10, Nov. 1988, pp. 2251.

[19] Mane, L., Loc, T.P, and Werle, H., "Sur le Décollement Instationnaire Autour d'un Profil á Grands Nombres de Reynolds : Une Comparison Calcul Expérience", *Mécanique des Fluides*, Académie des Scinces, 305, Seires II, 1987, pp. 229-232.

[20] Meier, G.E.A., "Private Communications"

Table 1: Experimental Conditions

M	α^+						
	0.01	0.02	0.025	0.03	0.035	0.04	0.05
0.20			X	X	X	X	X
0.25		X	X	X	X	X	X
0.30		X	X	X	X	X	
0.35		X	X	X	X	X	
0.40		X	X	X	X		
0.45	X	X	X	X			

Table 2: Vortex Release Angle of Attack

M	α^+							
	0*	0.01	0.02	0.025	0.03	0.035	0.04	0.05
0.20				17.5		21.0	22.0	24.0
0.25				17.5	18.5	21.0	22.0	27.0
0.3	12.4		17.5	18.0	20.0	21.0	23.0	
0.35	11.6		16.0	17.5	19.0	20.0	23.0	
0.40	10.8		15.5	17.0	19.0	20.0		
0.45	9.5	12.0	15.5	17.0	18.0			

* Best estimate of static stall angle from schlieren pictures.

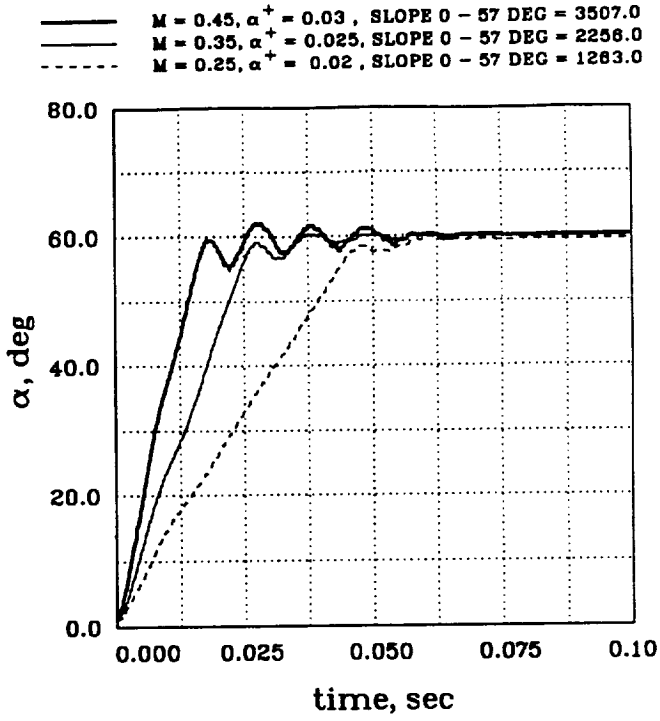

Fig. 2. Time History of Pitching Airfoil.

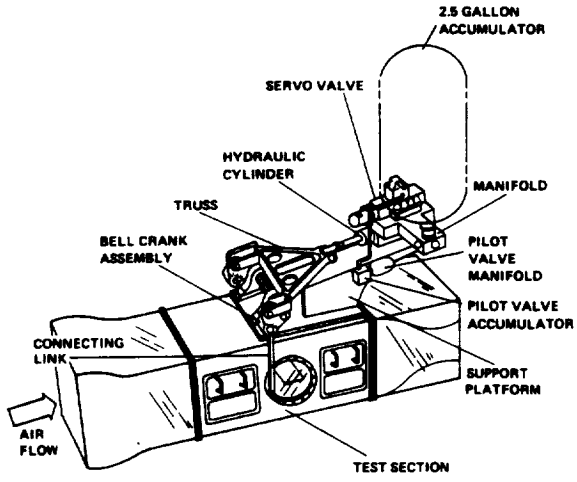

Fig. 1. Compressible Dynamic Stall Facility with a Hydraulic Drive.

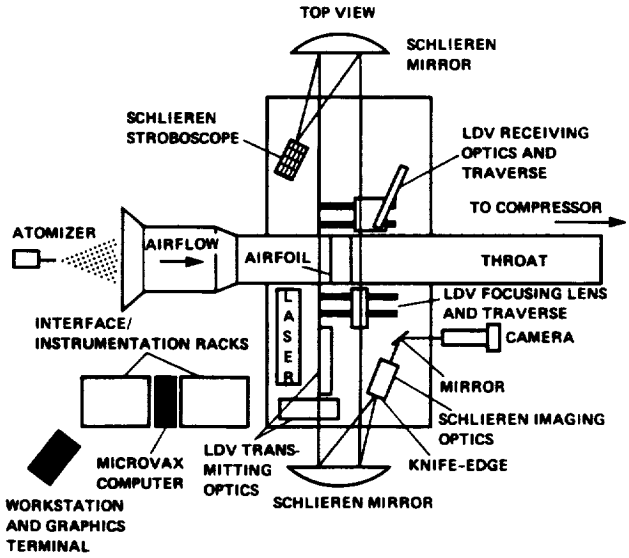

Fig. 3. Schematic of the CDSF Instrumentation.

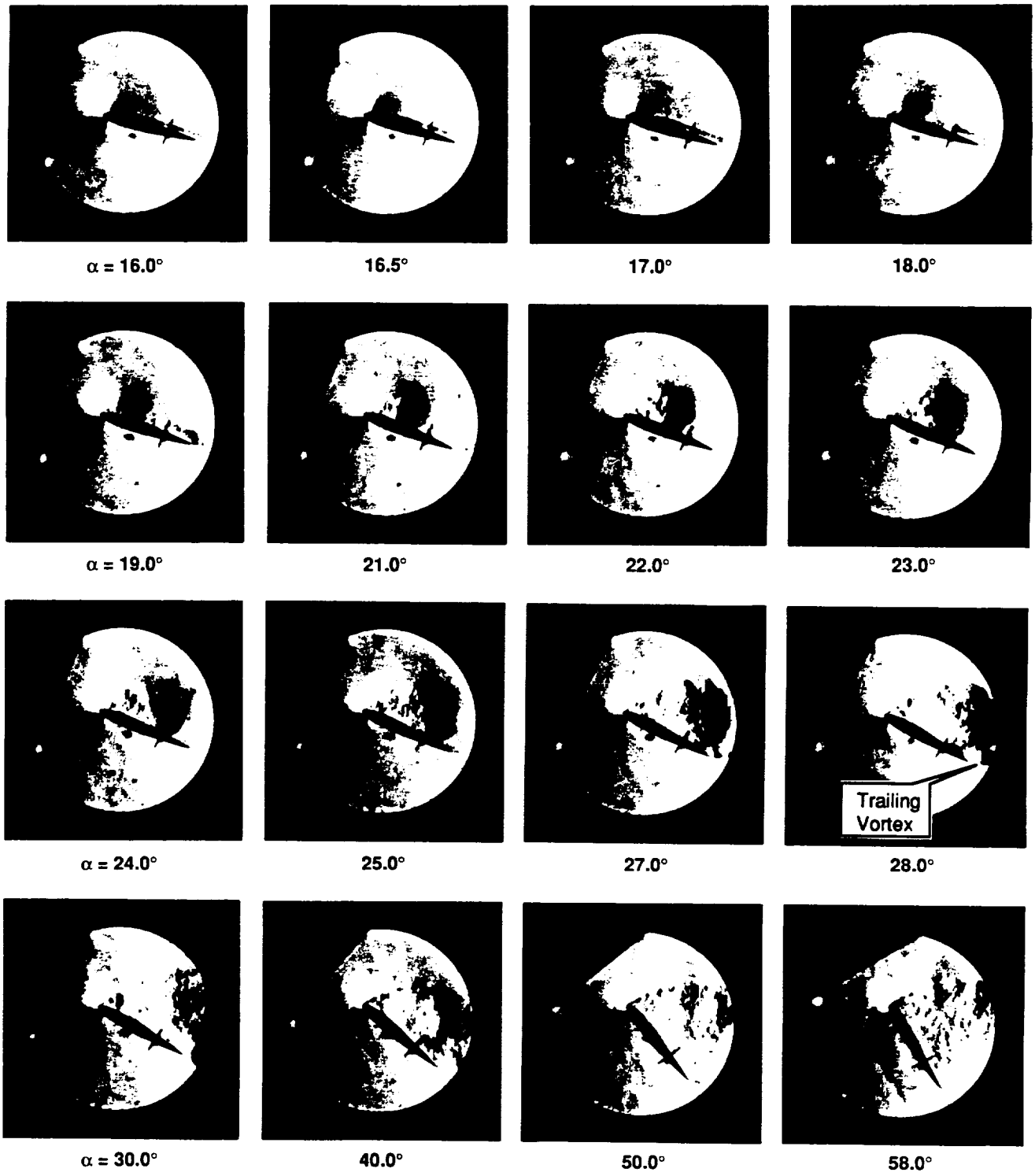

Fig. 4. Stroboscopic Schlieren Pictures of the Compressibility Effects on Dynamic Stall of a Rapidly Pitching Airfoil: M = 0.25, $\alpha^+ = 0.05$.

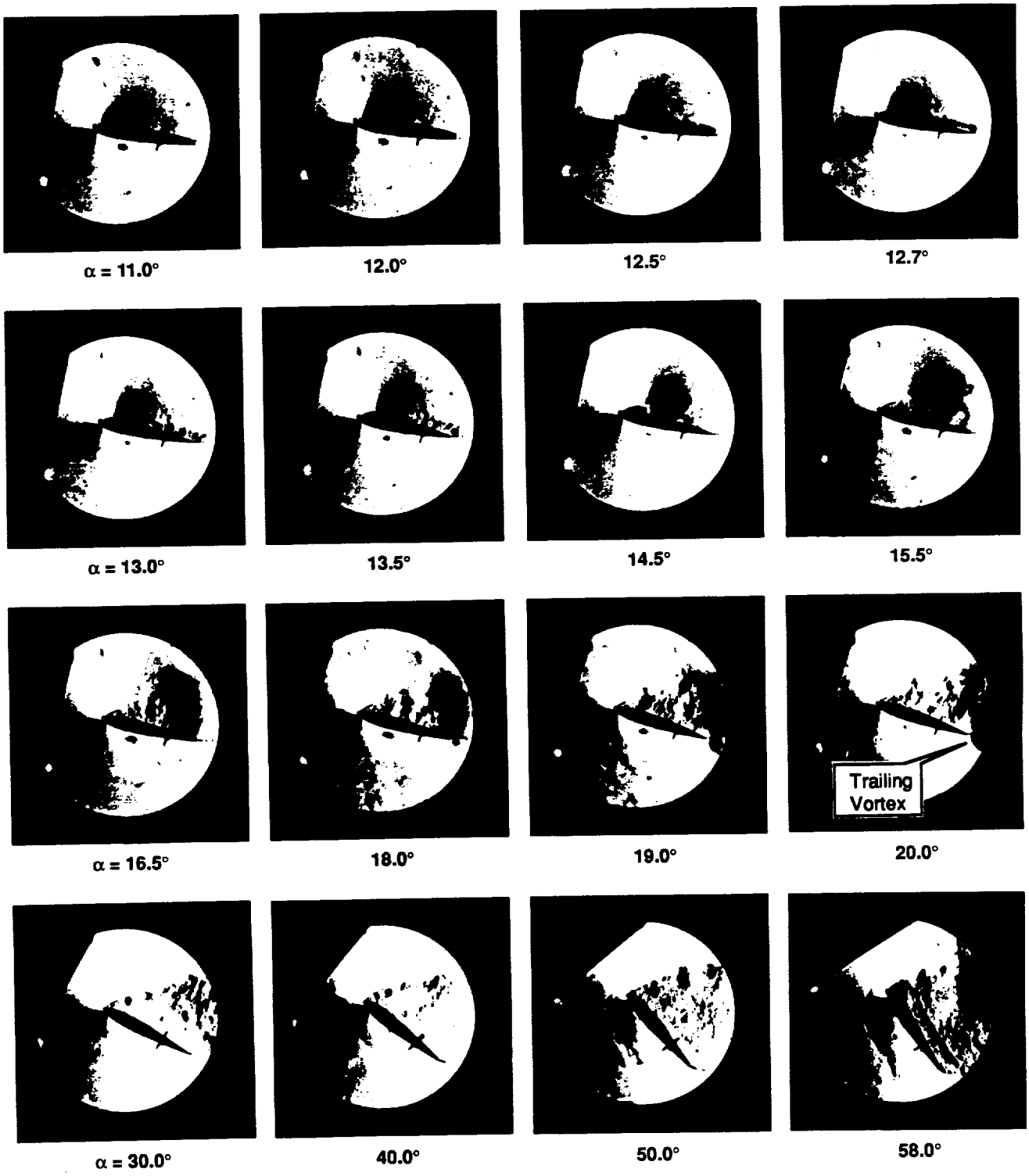

Fig. 5. Stroboscopic Schlieren Pictures of the Compressibility Effects on Dynamic Stall of a Rapidly Pitching Airfoil: M = 0.45, $\alpha^+ = 0.03$.

Fig. 6. Multiple Vortices on a Pitching Airfoil: M = 0.25, $\alpha^+ = 0.025$, $\alpha = 16.5^0$.

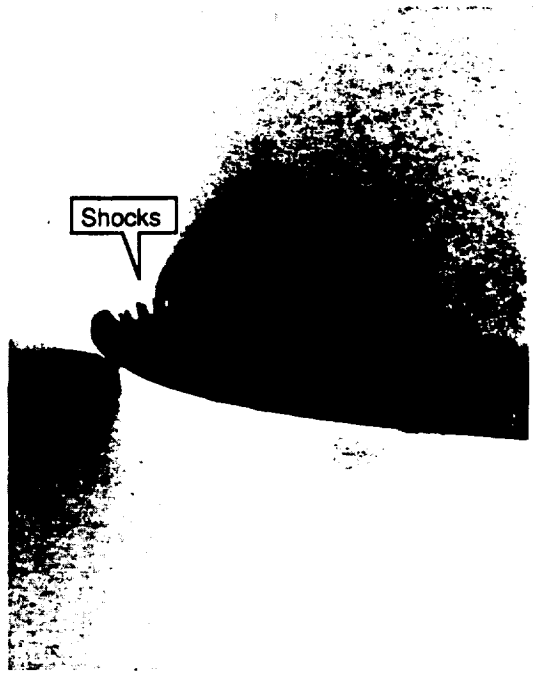

Fig. 7. Schlieren Pictures of Multiple Shocks on a Rapidly Pitching Airfoil: M = 0.45, $\alpha^+ = 0.0313$, $\alpha = 12.6^0$.

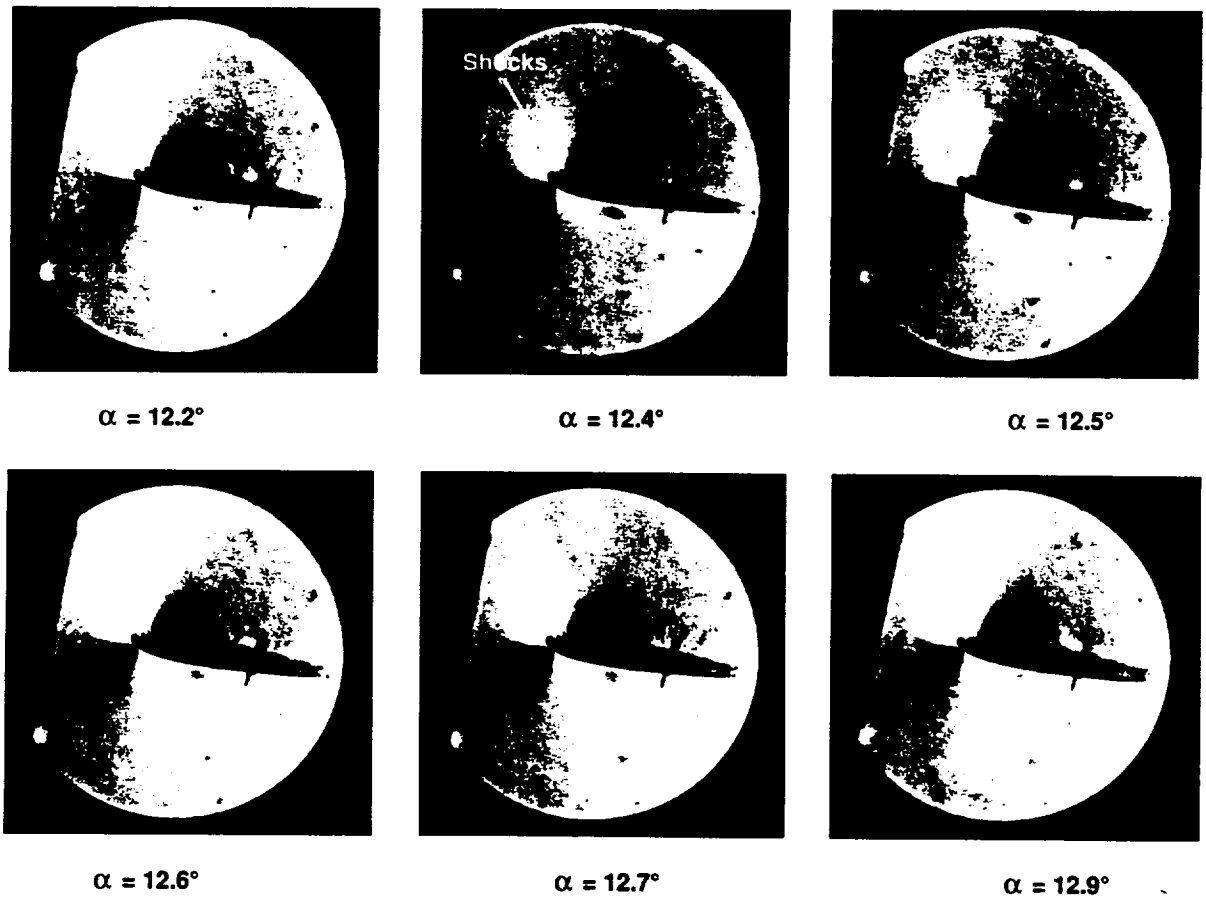

Fig. 8. A Sequence of Schlieren Pictures of Shocks on a Rapidly Pitching Airfoil: M = 0.45, $\alpha^+ = 0.0313$.

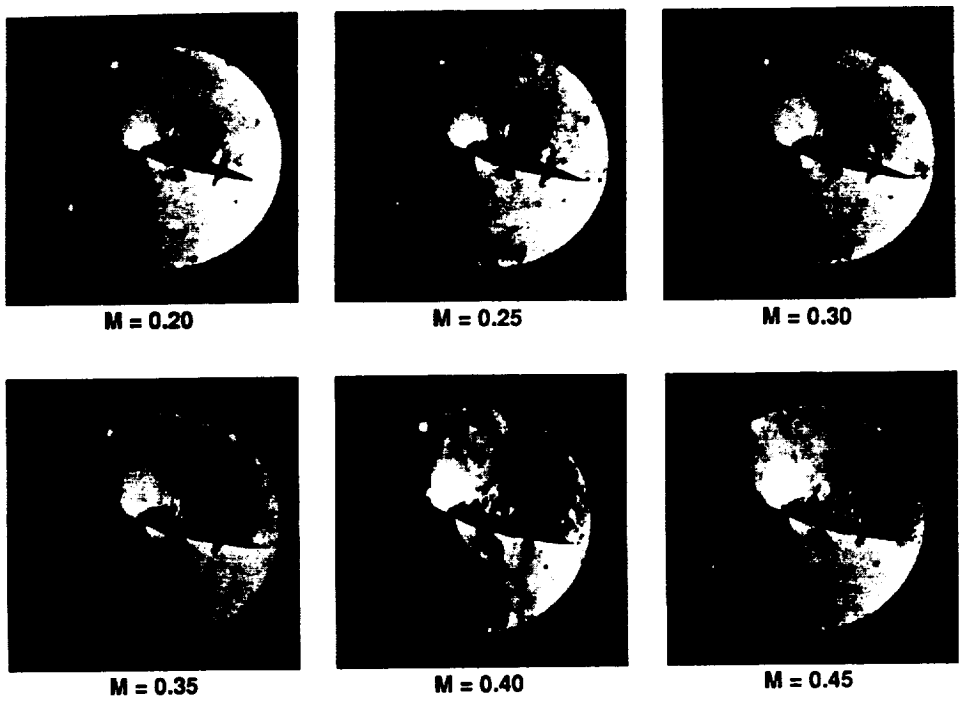

Fig. 9. Effect of Mach Number on Dynamic Stall of a Rapidly Pitching Airfoil, Schlieren Studies: $\alpha^+ = 0.03$, $\alpha = 17^0$.

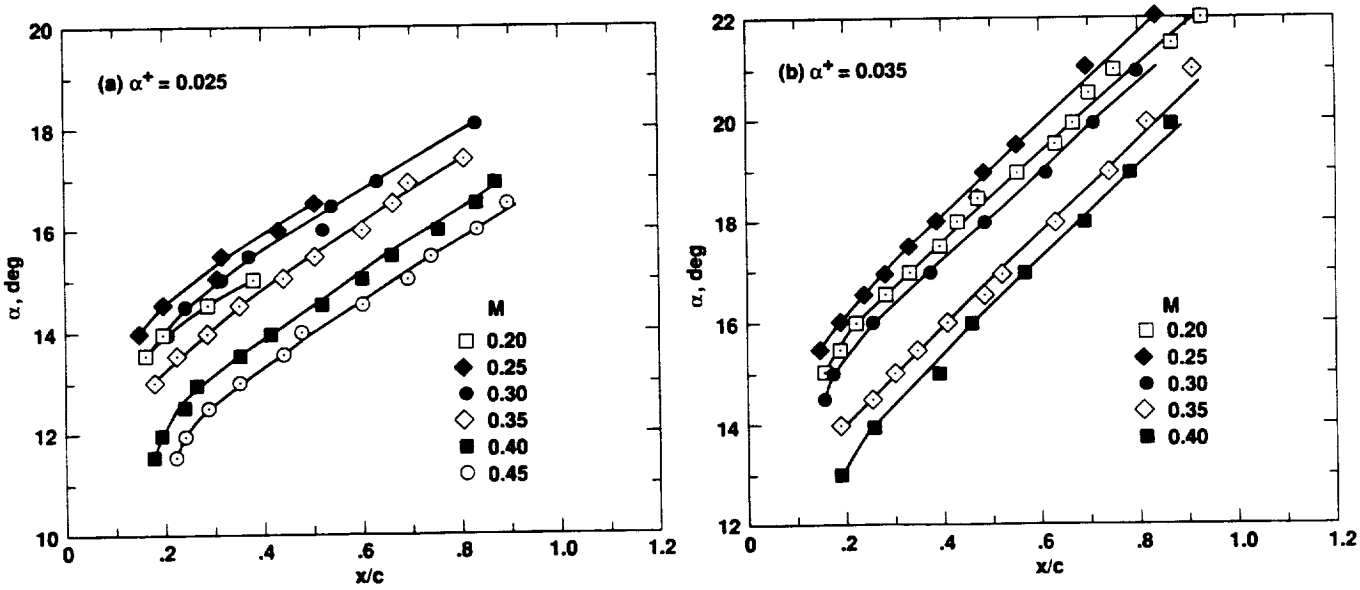

Fig. 10. Quantitative Effects of Mach Number on Dynamic Stall Vortex Location: (a) $\alpha^+ = 0.025$, (b) $\alpha^+ = 0.035$.

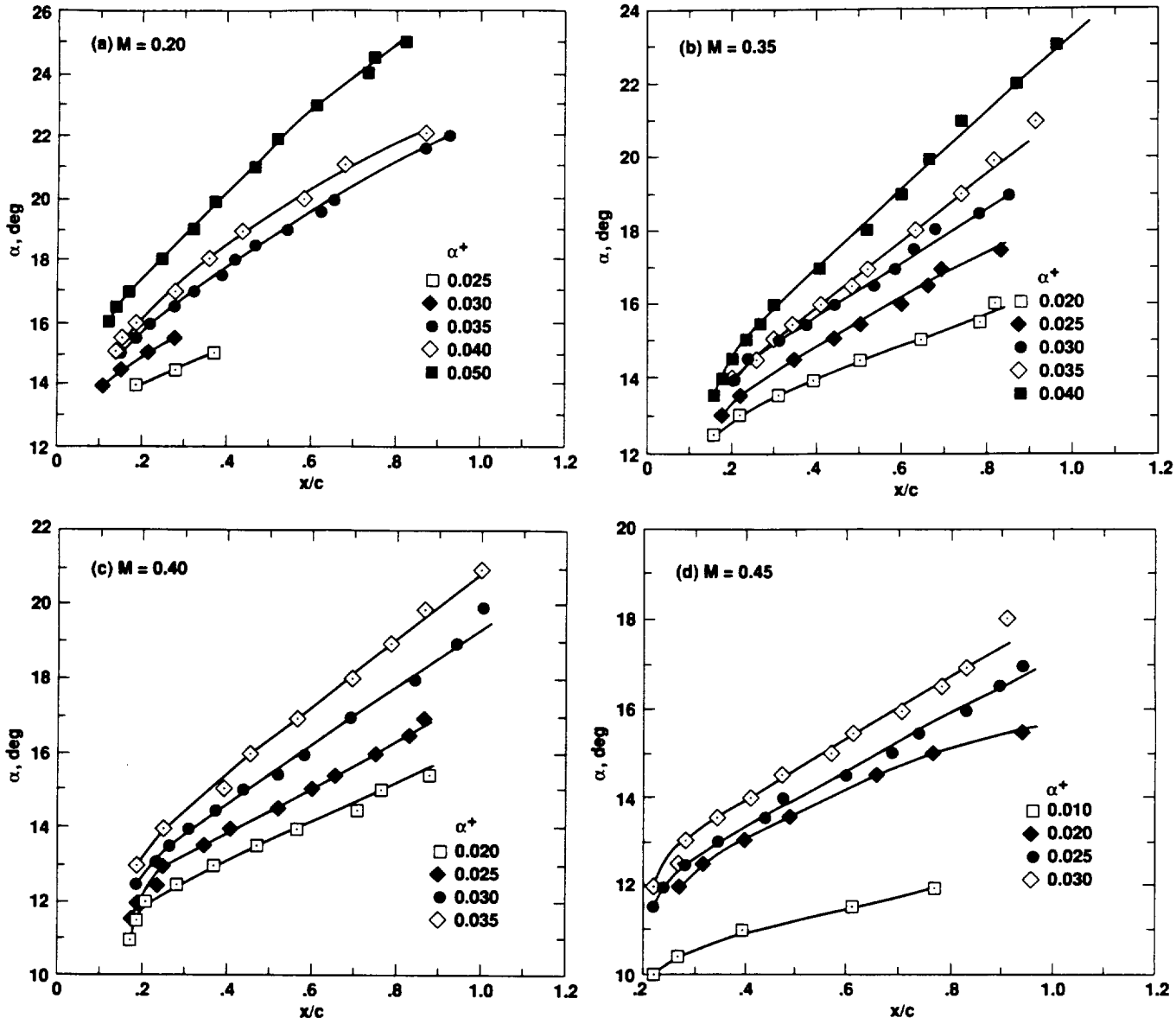

Fig. 11. Quantitative Effects of Pitch Rate on Dynamic Stall Vortex Location: (a) M = 0.2, (b) M = 0.35, (c) M = 0.40, (d) M = 0.45.

APPENDIX B